Assembly of Biomimetic Microreactors using Caged-Coacervate Droplets

Arjaree Jobdeedamrong,[†a,b] Shoupeng Cao,[†b] Iain Harley,[b] Daniel Crespy,[a] Katharina Landfester,[*b] and Lucas Caire da Silva[*b]

a Department of Materials Science and Engineering, School of Molecular Science and Engineering, Vidyasirimedhi Institute of Science and Technology, 21210 Rayong, Thailand

b Max Planck Institute for Polymer Research, Ackermannweg 10, 55128, Germany.

Email of corresponding authors:

silva@mpip-mainz.mpg.de
landfester@mpip-mainz.mpg.de

Supporting Information

1. Materials

Tetraethyl orthosilicate (TEOS, Acros Organics, 98%), chloroform ($CHCl_3$, Carlo Erba, 99%), dimethyloctadecyl[3-(trimethoxysilyl)propyl]ammonium chloride (TPOAc, ACROS, 60% in methanol), hexadecane (HD, Acros Organics, 99%), chloro-2-hydroxypropyltrimethylammonium chloride (Sigma, 60% in water), phosphate buffered saline (PBS, Sigma Aldrich), Calcein (mixed isomers, Sigma), PEG-methoxysilane (Rapp-polymer), Fluorescein isothiocyanate-polyethylene glycol (FITC-PEG, M_w = 1 kDa, Creative PEGWorks), Fluorescein isothiocyanate-dextran (FITC-dextran, M_w = 4 kDa, 10 kDa, or 20 kDa, Sigma), Nile red (Sigma, >97%), amylose (Biosynth Carbosynth), glucose oxidase from Aspergillus niger (GOx, Type X-S, lyophilized powder, 100,000-250,000 units/g solid, G7141-50KU, Sigma Aldrich), and peroxidase from horseradish (HRP, Type II, essentially salt-free, lyophilized powder, 150-250 units/mg solid, P8250-50KU, Sigma Aldrich) were used as received. Deionized water was used through all the experiments.

2. Synthesis of quaternized amylose (Q-AM)

Quaternized amylose and carboxy-functionalized amylose were prepared according to previous reports.[1] Quaternized amylose was prepared by dissolving 1.5 g amylose and 2.8 g NaOH in 14 mL Milli-Q at 30 °C. After complete dissolution of the amylose, 11.6 mL of 3-chloro-2-hydroxypropyltrimethylammonium chloride solution (60 wt% in water) was added

dropwise into the stirring reaction mixture, which was subsequently left to react overnight. After this time, the mixture was neutralized with acetic acid and precipitated into 200 mL cold ethanol. The resulting precipitate was re-dissolved in Milli-Q water and dialyzed extensively against water using regenerated cellulose dialysis tubing (Spectrum Labs, USA) with a MWCO of 3.5 kDa before lyophilization. ^{1}H NMR spectroscopy (D_2O) characterization data and chemical structures are presented in Fig. S1.

Carboxy-functionalized amylose was prepared by dissolving 1.5 g amylose and 3.6 g NaOH in 15 mL Milli-Q at 70 °C. After complete dissolution of the amylose, 2.7 g chloroacetic acid was added and the reaction mixture was left to stir for 2 h. After the reaction, the mixture was neutralized with acetic acid and precipitated into 200 mL cold ethanol. The resulting precipitate was re-dissolved in Milli-Q water and dialyzed extensively against water using regenerated cellulose dialysis tubing (Spectrum Labs, USA) with a MWCO of 3.5 kDa before lyophilization. ^{1}H NMR spectroscopy (D_2O) characterization data and chemical structures are presented in Fig. S1.

3. Synthesis of ultrasmall silica nanocapsules (ul-SiO_2NCs)

Firstly, an aqueous phase and an oil phase were prepared separately. TEOS (2.14 mL), Nile red (1 mg), and chloroform (0.100 mL) were dissolved in 0.543 mL cyclohexane and mixed with 30 mL of a 0.38wt% aqueous solution of TPOAC. The mixture was stirred at 540 rpm for 10 min and processed by ultrasonication (50% amplitude in a pulsed regime, 3 min, 3 s pulse, and 1 s pause) under ice-cooling. The resulting miniemulsions were stirred for 20 h at 25 °C and then stirred for 6 h at 40 °C to obtain ultrasmall silica nanocapsules.

4. Synthesis of large silica nanocapsules (L-SiO_2NCs)

TEOS (2.14 mL), Nile red (1 mg), and hexadecane (125 mg) were dissolved in 2.0 mL chloroform and mixed with 30 mL of a 0.38wt% aqueous solution of TPOAC. The mixture was stirred at 540 rpm for 10 min and processed by ultrasonication (50% amplitude in a pulsed regime, 3 min, 3 s pulse, and 1 s pause) under ice-cooling. The resulting miniemulsions were stirred for 20 h at 25 °C and then stirred for 6 h at 40 °C to obtain large silica nanocapsules.

5. PEGylation of silica nanocapsules (PEG-SiO_2NCs)

2.5 mL of SiO_2NCs dispersion was mixed with 1 mL of 60 mg/mL (for ul-SiO_2NCs) or 30 mg/mL (for L- SiO_2NCs) PEG-methoxysilane aqueous solution then, the mixture was stirred

for 24 h at 300 rpm, 25 °C. The resulting solution was purified by dialysis bag (MWCO = 1 kDa) against DI water for 2 days.

6. Formation of caged-coacervates

100 µL of 1mg/mL C-Am in PBS solution was mixed with 200 µL of 1mg/mL Q-Am in PBS solution by stirring at 200 rpm. Then, 150 µL of PEG-SiO_2NCs (0.5wt%) dispersion was added to the coacervate dispersion. The mixture was stirred at 200 rpm for 3 min to obtain SiO_2NCs caged-coacervates. For encapsulation of enzymes in coacervates, the enzymes were pre-dissolved in a Q-Am aqueous solution. 30 µL of 0.4 mg/mL GOx and 30 µL of 0.0025mg/mL HRP in PBS solution were mixed with 200 µL of 1mg/mL Q-Am in PBS solution. Formation of coacervate was achieved following the described procedure. 100 µL of 1mg/mL C-Am in PBS solution was added in 200 µL of 1mg/mL Q-Am in PBS solution containing GOx and HRP. The mixture was stirred at 200 rpm. Then, 150 µL of PEG-SiO_2NCs (0.5%w/w) dispersion was mixed with coacervate solution by stirred at 200 rpm for 3 min to obtain SiO_2NCs Pickering coacervates loading enzymes.

7. Permeability test

20 µL of coacervate suspension was dispersed in 200 µL of 20 µg/mL calcein in PBS or 100 µg/mL FITC-PEG and FITC-dextran in PBS. The fluorescence intensity of dyes in coacervates was investigated by confocal laser scanning microscopy (Leica TCS 264 SP5X system)

8. Enzymatic cascade in caged-coacervates

5 µL of 50 mM glucose in PBS and 3 µL of 1 mM Amplex Red in PBS were added in 150 µL of caged-coacervate dispersion containing GOx and HRP. CLSM images and videos were acquired using a Leica TCS SP5 II system.

9. Characterization of SiO_2NCs

The average size and morphology of SiO_2NCs were determined with a Jeol 1400 (Jeol Ltd, Tokyo, Japan) transmission electron microscope (TEM) operating at an accelerating voltage of 120 kV. Samples for TEM were prepared by drop casting the diluted dispersions (solid content: ~ 0.002 wt%) on carbon layer-coated copper grids. Zeta potential measurements were performed with diluted dispersions in a 10^{-3} M potassium chloride solution at pH 6.8 (dilution factor = 20) and 25 °C with a Malvern Zeta sizer (Malvern Instruments, UK). The solid content

of SiO_2NCs dispersion was measured by gravimetry after freeze-drying the dispersion. The amount of PEG on SiO_2NCs was determined by NMR spectroscopy in a Bruker Avance 250 MHz and 300 MHz.

10. Cryo-TEM imaging of the caged coacervates

3µl of caged coacervates stabilized by 10 nm silica nanocapsules was transferred to a glow-discharged 300 mesh 2/1 Quantifoil grid and then blotted for 2.5s at 100% humidity at 21°C using a Vitrobot Mark before plunge-freezing with liquid ethane. The grid was loaded into a Titan G4 Cryo-TEM and imaged in EFTEM mode with Gatan K3.

11. Supporting figures

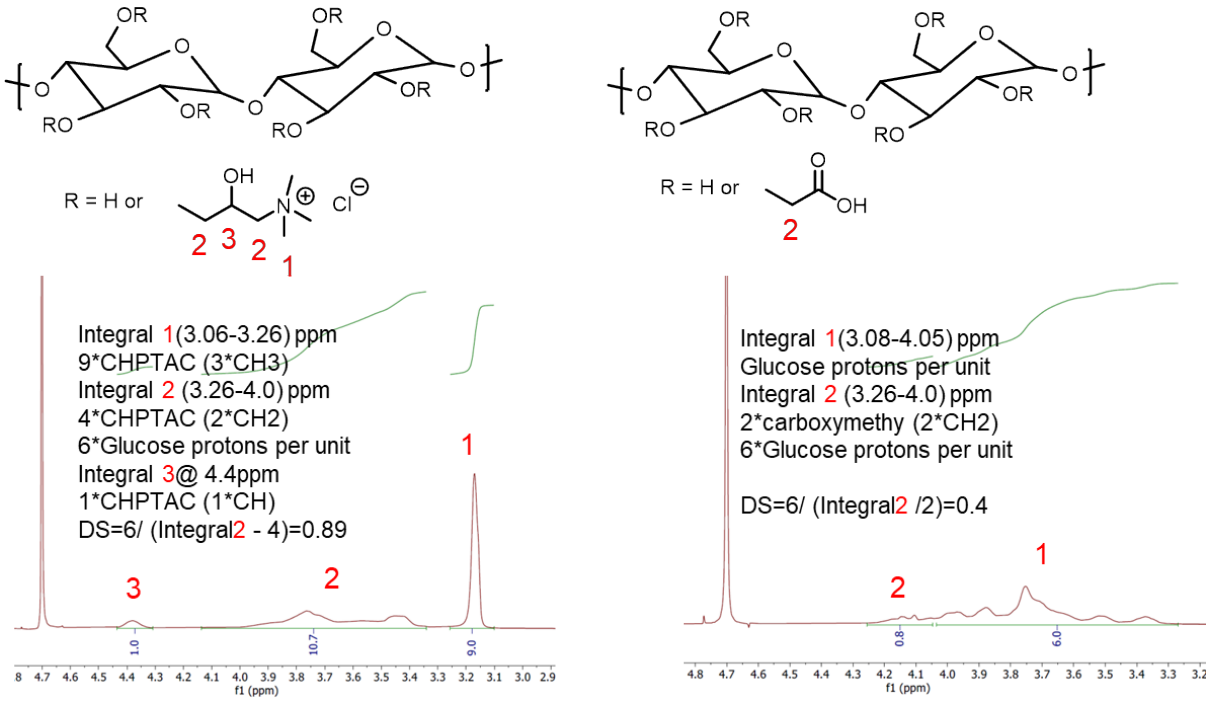

		Mean (mV)	Area (%)	St Dev (mV)
Zeta Potential (mV): 21.0	Peak 1:	21.0	100.0	4.68
Zeta Deviation (mV): 4.68	Peak 2:	0.00	0.0	0.00
Conductivity (mS/cm): 2.84	Peak 3:	0.00	0.0	0.00

Result quality : Good

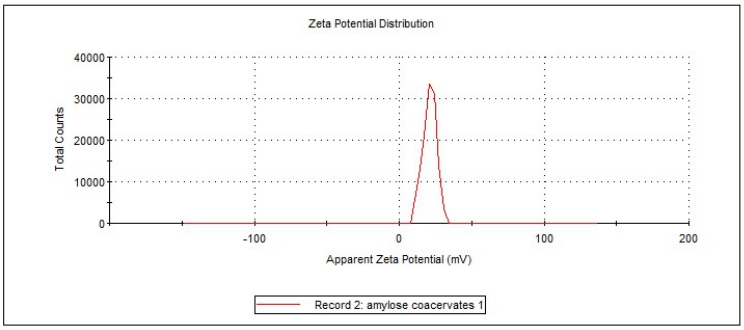

Fig. S1. Top: ^{1}H NMR spectra of quaternized and carboxymethylated amylose with their degree of substitution (DS = number of modifying groups per glucose unit). Bottom: Zeta-potential measurement of 2:1 Q-Am/Cm-Am coacervate droplets in 20-fold diluted PBS.

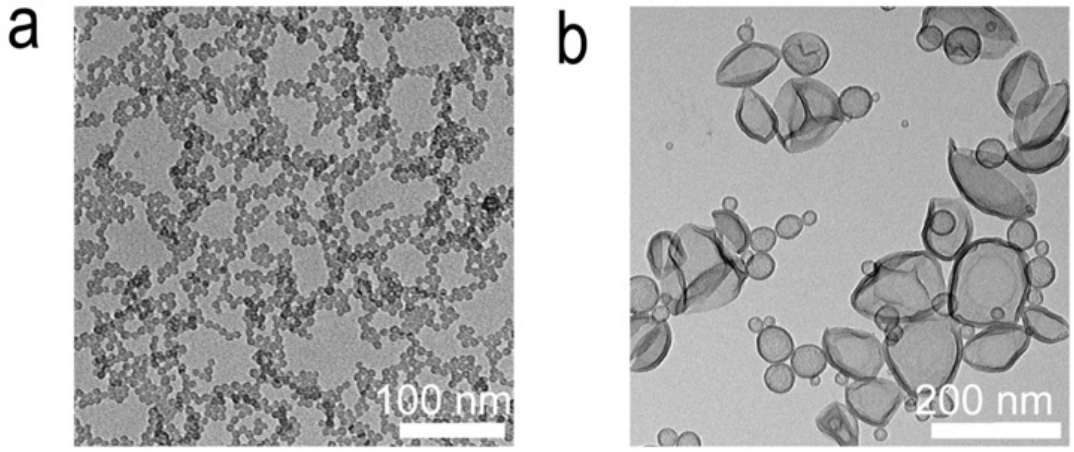

Fig. S2. TEM micrographs of SiO_2NCs with 10 nm (a) and 100 nm (b).

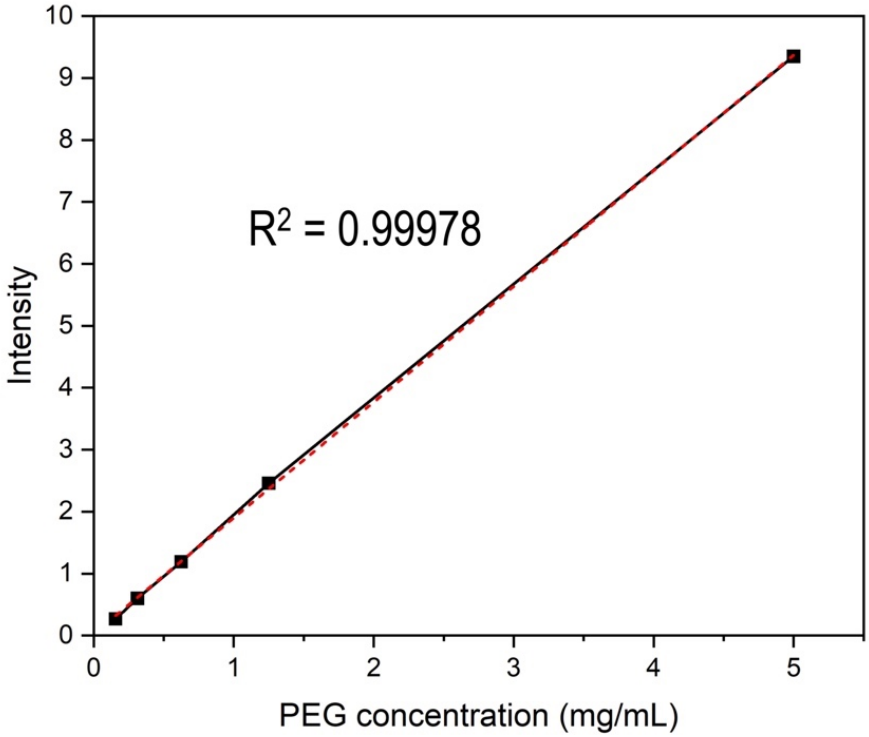

Fig. S3. Calibration curves for the determination of polyethylene glycol content on the shell of silica nanocapsules by^{1}H NMR spectroscopy at 3.52 ppm.

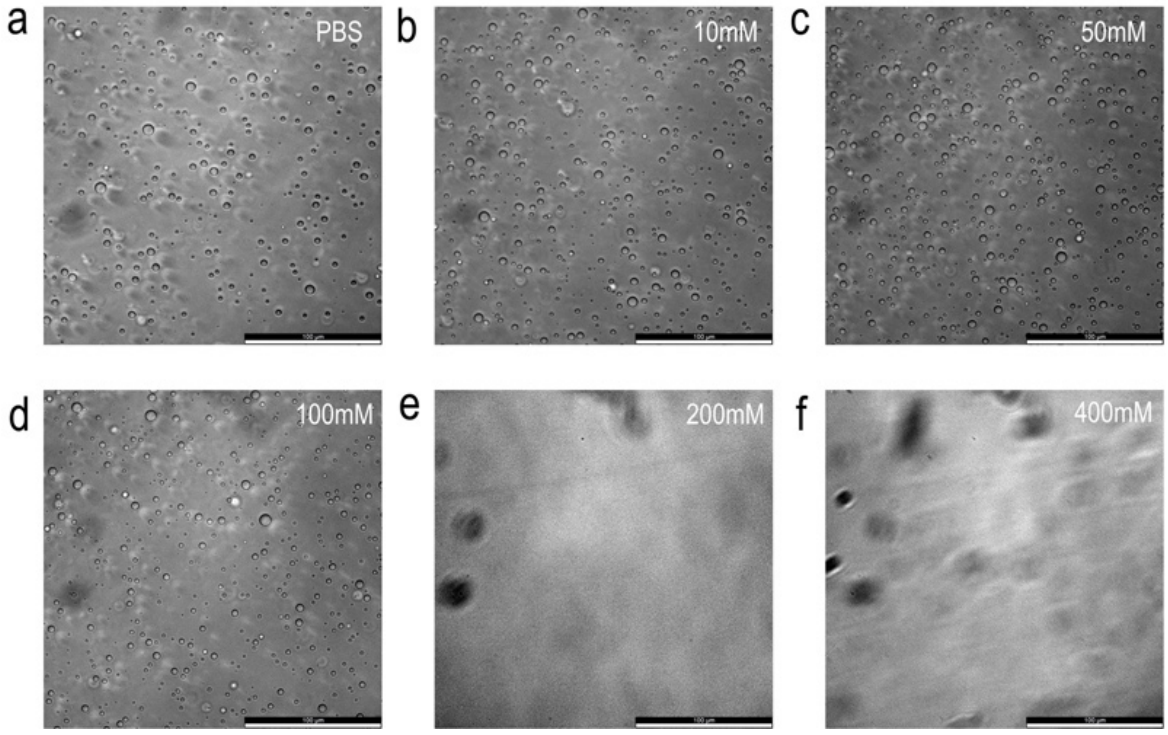

Fig. S4. Bright field images of Pickering coacervates stabilized by PEG-ul-SiO_2NCs in 0 (a), 10 (b), 50 (c), 100 (d), 200 (e), and 400 (f) mM sodium chloride aqueous solutions.

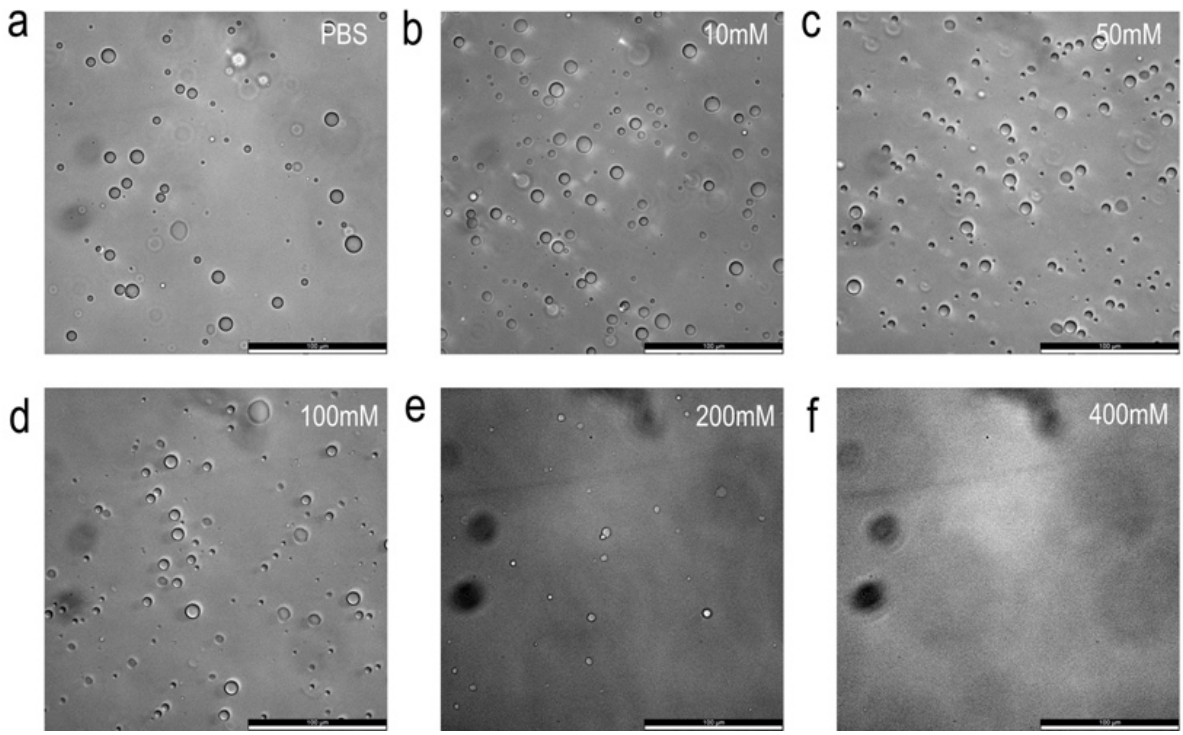

Fig. S5. Bright field images of Pickering coacervate stabilized by PEG-L-SiO_2NCs in 0 (a), 10 (b), 50 (c), 100 (d), 200 (e), and 400 (f) mM sodium chloride aqueous solutions.

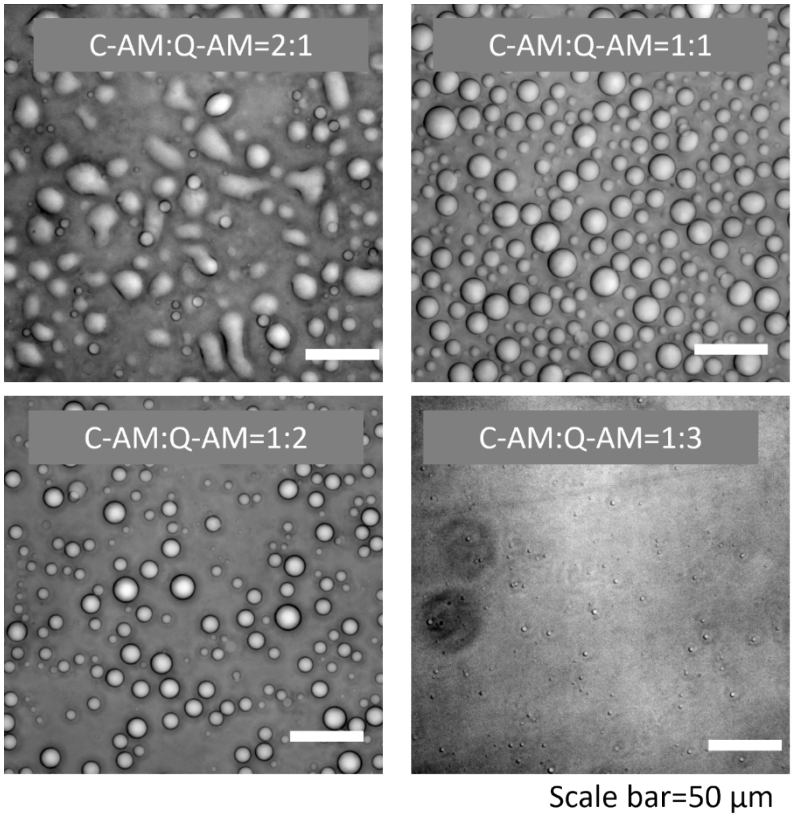

Sample	Zeta Potential (mV)	St Dev (mV)
2:1	-20.4	2.15
1:1	6.03	0.73
1:2	13.8	1.05
1:3	10.6	1.22

Fig. S6. Bright field images and zeta potential measurements of Pickering coacervates formed with different ratio of C-AM and Q-AM. Samples stabilized by silica nanocapsules (100 nm). Stable droplets were observed for C-AM and Q-AM at 1:1 and 1:2. An excess of C-AM or Q-AM formed coacervates rapidly coalesce. The zeta potential shows that an increasing ratio of the positively charged Q-AM produces a corresponding increase in the surface charge of the coacervates.

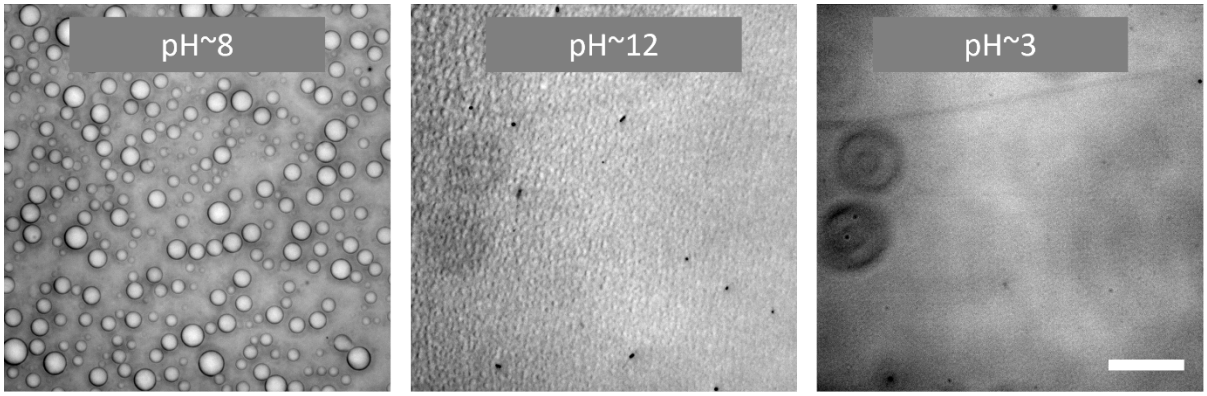

Fig. S7. Caged-coacervates stabilized with silica nanocapsules were exposed to different pH values. The bright images show that the caged-coacervates are relatively stable at a pH of 8, but disintegrate into very small droplets at a pH of 12. The coacervates completely dissolved at pH 3, due to the protonation of C-AM, which reduces the electrostatic interaction with C-AM.

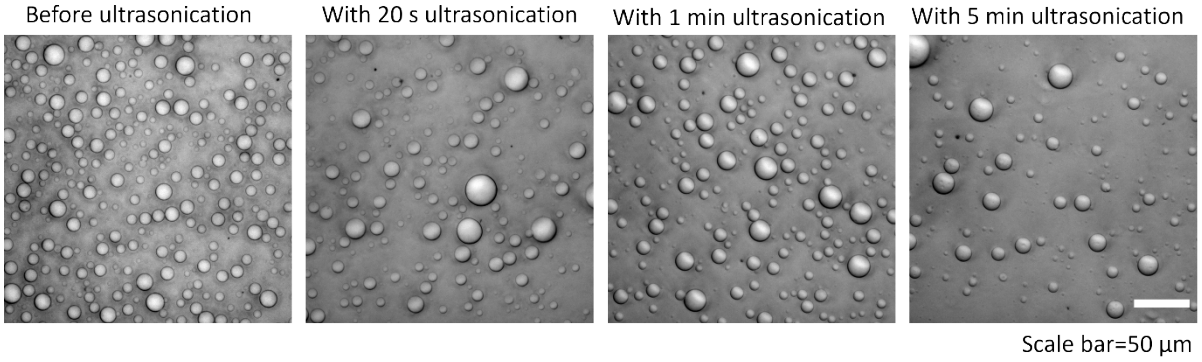

Fig. S8. Caged-coacervates are relatively stable even after ultrasonic treatment. Bright-field microscopy images showed that a considerable amount of coacervates can still be seen after 5 minutes of ultrasound treatment, which underlines their robustness.

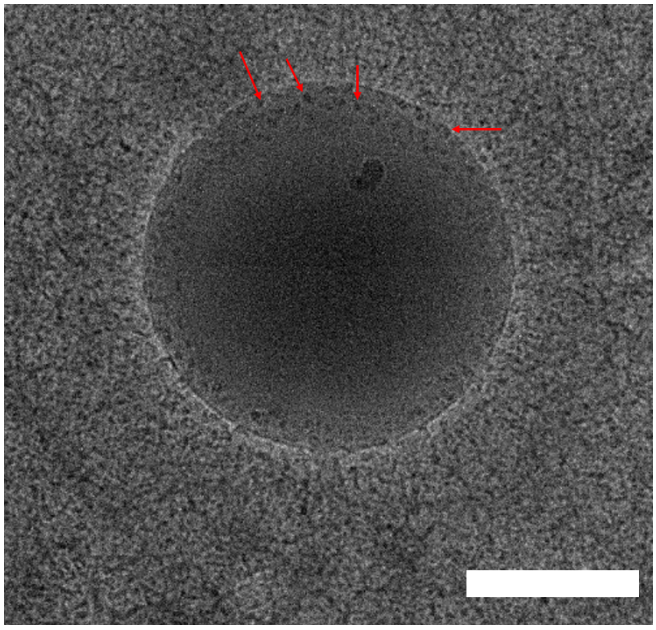

Fig. S9. Cryo-TEM image of the Pickering coacervates that are stabilized by 10 nm silica nanocapsules. The red arrow indicates the position of the silica nanocapsules.

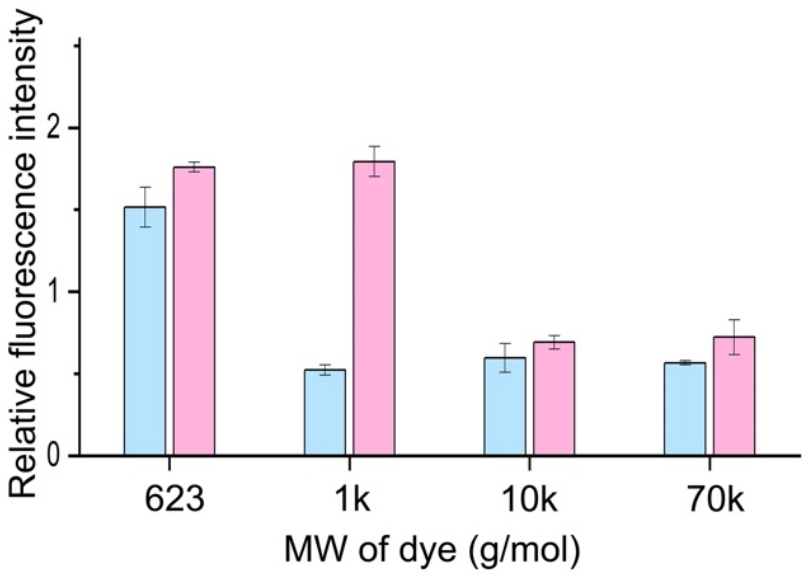

Fig. S10. Relative fluorescence intensity of the coacervates stabilized with PEG-SiO_2NCs 10 nm (blue bar), and 100 nm (pink bar), compared with the fluorescence intensity of background.

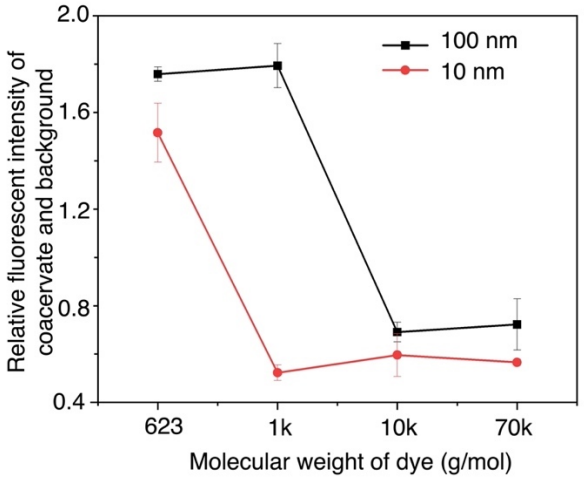

Fig. S11. Relative fluorescence intensity of caged coacervates stabilized with PEG-SiO_2NCs 10 nm (red line), and 100 nm (black line), compared with the background fluorescence intensity.

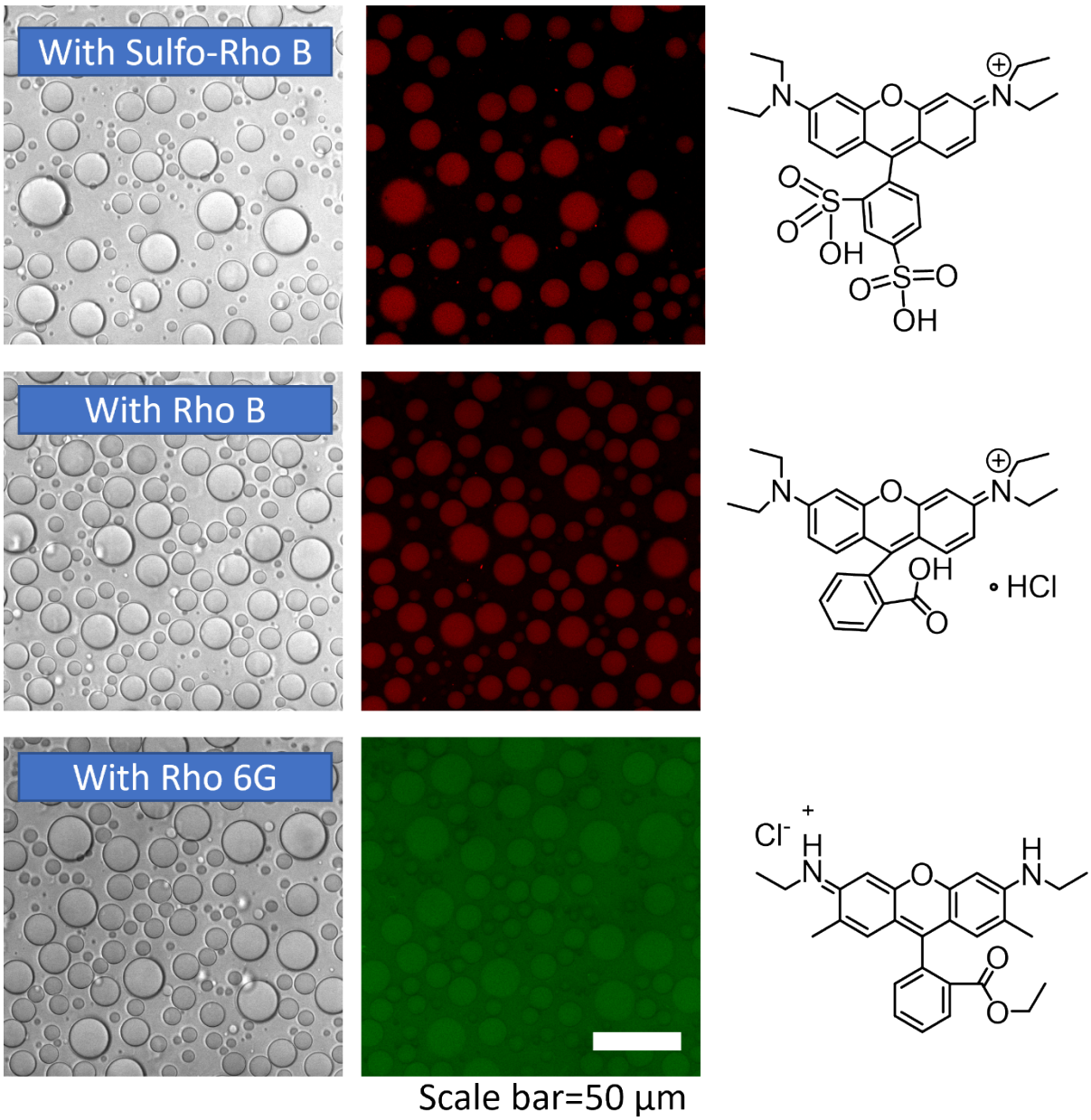

Fig. S12. Different small molecules such as sulfo-rhodamine B, Rhodamine B and Rhodamine 6G are encapsulated. The caged-coacervates can effectively sequestrate negatively charged or zwitterionic cargoes as indicated by the high contrast between the fluorescence intensity inside the coacervate and the external medium. The positively charged Rhodamine 6G is not efficiently sequestrated, as indicated by similar intensities of the dye inside and outside the microdroplets. These observations illustrate the selectivity of coacervates towards different cargoes, which cannot be easily achieved by conventional hollow compartments.

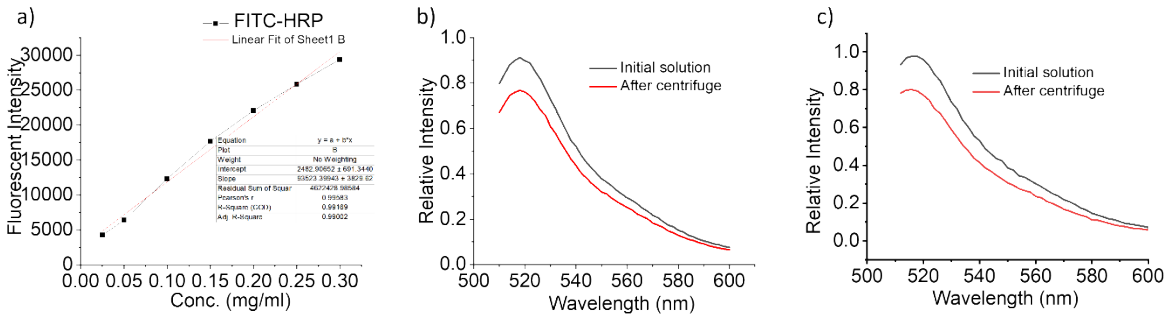

Fig. S13. a) Calibration curve of FITC-HRP used in the determination of the enzyme loading efficiency in caged-coacervates. b) Relative emission intensity of Pickering coacervates (with 100 nm NCs) before and after centrifugation and re-dispersion. c) Relative emission intensity of caged-coacervates (10 nm NCs) before purification and caged-coacervates after purification. Loading efficiency of HRP: 78.3% (100 nm NCs) and 76.3% (10 nm NCs)

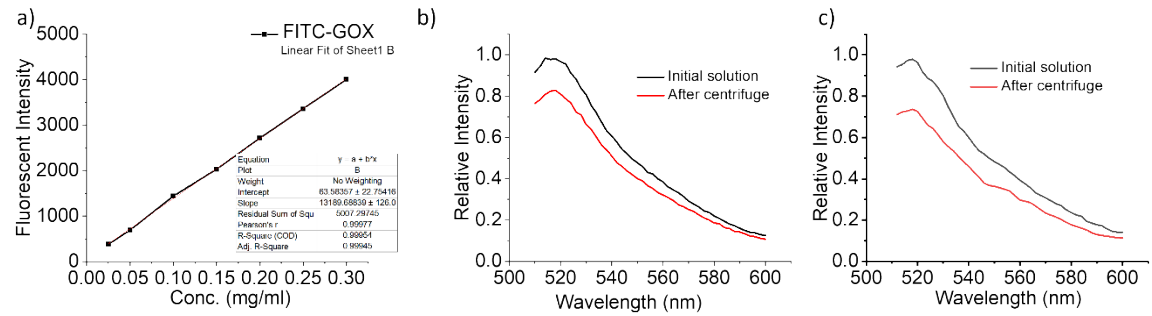

Fig. S14. a) Calibration curve of FITC-GOX used in the determination of the enzyme loading efficiency in caged-coacervates. b) Relative emission intensity of Pickering coacervates (with 100 nm NCs) before and after centrifugation and re-dispersion. c) Relative emission intensity of caged-coacervates (10 nm NCs) before purification and caged-coacervates after purification. Loading efficiency of GOX: 83.2 (100 nm NCs) and 71.4% (10 nm NCs).

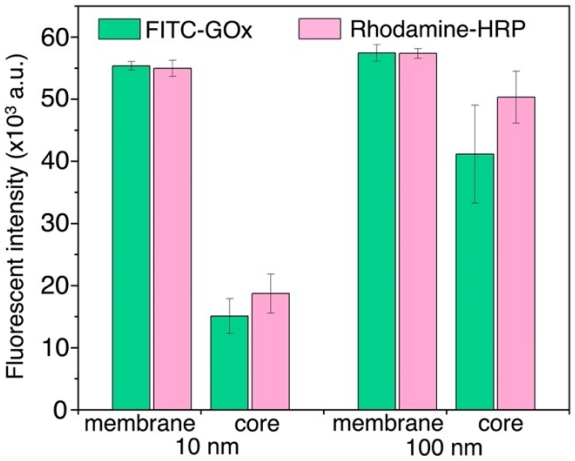

Fig. S15. Fluorescent intensity of FITC-GOx (green bar) and Rhodamine-HRP (pink bar) at distinct locations in coacervates stabilized with PEG-SiO_2NCs 10 and 100 nm. Determined by confocal laser microscopy.

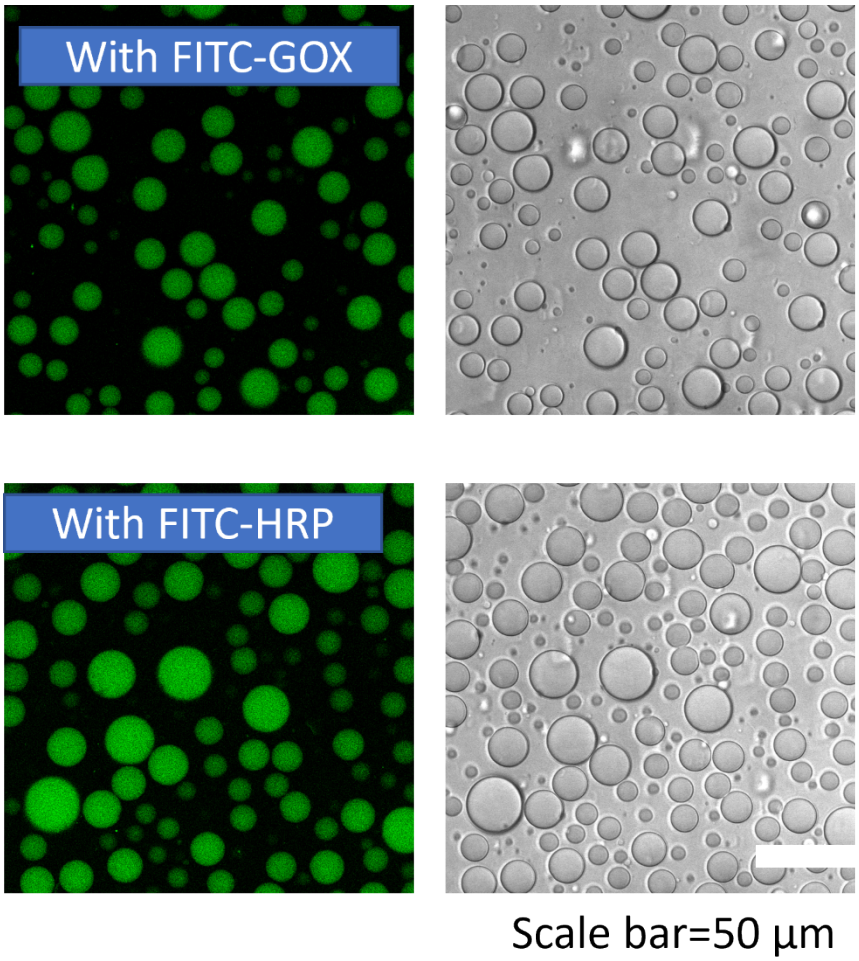

Fig. S16. The partition coefficient of FITC-GOX and FITC-HRP was determined by image analysis of confocal micrographs. The values were 42.4±11.4, and 50.2±10.1 respectively.

Reference

[1] A. F. Mason, B. C. Buddingh', D. S. Williams, J. C. M. van Hest, *J. Am. Chem. Soc.* **2017**, *139*, 17309-17312.